

# CURVE VEERING IN THE EIGENVALUE PROBLEM OF ROTOR-BEARING SYSTEMS

Yang-Gyu Jei\* and Chong-Won Lee\*\*

(Received March 7, 1990)

When the eigenvalues approach each other as system parameters vary, they often cross (curve cross) or abruptly veering (curve veering). An important characteristic of the curve veering in the eigenvalue problem is that the mode shapes associated with eigenvalues before veering are abruptly change during veering in a rapid but continuous way. In this paper, the existence of the curve veering in the eigenvalue problem of general rotor-bearing systems including the effects of rotary inertia and gyroscopic moments is verified by modal analysis and perturbation technique. The criteria of the curve veering are derived as bearing stiffness and rotational speed vary. The abrupt but continuous changes of mode shapes during veering are also illustrated.

**Key Words :** Curve Veering, Eigenvalue Problem, Eigenvalue, Mode Shape, Whirl Speed, Perturbation Technique, Anisotropic Rotor-Bearing System, Asymmetrical Rotor-Bearing System

## 1. INTRODUCTION

When eigenvalues are plotted against a system parameter, the dependence of eigenvalues on the system parameter is illustrated by a family of loci. When two loci approach each other, they often cross or abruptly diverge. The latter case is often called curve veering, during which mode shapes rapidly change. The existence of curve veering has already been investigated in the some literature (Classen and Thorne, 1962 ; Leissa, 1974 ; Kuttler and Sigillito, 1981 ; Schajer, 1984), but the phenomenon has not been universally accepted. The rapid change in mode shapes during veering has doubt on the validity of approximate solutions. In 1974, Leissa raised the question of whether curve veering occurs because of the mathematical models or results from the approximation method used to estimate the frequencies. But the existence of curve veering was recently verified by obtaining exact solution of the continuous model for a rotating, guided, circular string (Perkins and Mote, 1986).

Although the name of the curve veering in the eigenvalue problem of rotor-bearing systems has not been found, the curve veering phenomenon was already shown in the literature in the field of rotor dynamics (Yamamoto and Ōta, 1964 ; Dimentberg, 1961 ; Crandall and Yeh, 1989). In Crandall and Yeh's words (1989) "It is interesting that when the curve for an even rotor mode approaches the curve for an even stator mode, or an odd rotor mode approaches an odd stator mode, the two modes form a coupled system and the curves repel each other avoiding an intersection" in the Campbell diagram of the natural frequency of a uniform rotor

rotating in a uniform stator as function of rotational speed.

But since no attention was paid to mode shapes, the significance of the curve veering could not be noticed. An important characteristic of the curve veering is that the mode shapes associated with the eigenvalues before veering are interchanged during veering in a rapid but continuous way. The information of mode shapes as well as eigenvalues is important for the rotor dynamic analysis (Jei and Lee, 1987 ; Lee and Jei, 1988 ; Jei and Lee, 1989).

Modal analysis of a continuous rotor-bearing system including the effects of gyroscopic moment, rotary inertia and natural boundary conditions was performed (Jei and Lee, 1987 ; Lee and Jei, 1988). The exact solution methods were also developed, and various vibration characteristics such as whirl speeds, mode shapes, forced responses and stabilities were investigated. In this paper the curve veering in the eigenvalue problem of rotor-bearing systems is verified using the modal analysis and exact solution methods developed by authors (Jei and Lee, 1987 ; Lee and Jei, 1988) and the perturbation technique developed by Perkins and Mote (1986). As bearing stiffness and rotational speed vary, the criteria of the curve veering are derived. The abrupt but continuous changes in mode shapes during veering are also illustrated.

## 2. CURVE VEERING IN THE EIGENVALUE PROBLEM OF ROTOR SYSTEMS

Some analytical solutions for the transverse vibration analysis of distributed parameter rotor systems were provided, and modal analyses were performed, but most works have considered only simple models such as Euler-Bernoulli shafts under geometric boundary conditions. Such rotor systems are essentially non-rotating systems. The difficulties in modal analysis of rotor-bearing systems which include the effects of rotary inertia and gyroscopic moments arise from the fact that the resulting eigenvalue problems are characterized by

\*Senior Researcher, Shafting and Rotor Dynamics Laboratory Korea Research Institute of Ships and Ocean Engineering, Daejeon 305-606, Korea.

\*\*Department of Mechanical Engineering, Korea Advanced Institute of Science and Technology, Seoul 130-650, Korea

the presence of skew symmetric matrices with differential operators as elements, due to rotation and/or damping, resulting in non-self adjoint eigenvalue problem. By writing the equation of motion in state space rather than configuration space the standard non-self adjoint eigenvalue problem of distributed parameter rotor systems which include the effects of gyroscopic moments and rotary inertia was formulated (Jei and Lee, 1987; Lee and Jei, 1988).

The eigenvalue problem associated with an anisotropic rotor-bearing system which consists of rigid disks, discrete anisotropic bearings and non-uniform Rayleigh shafts or an asymmetrical rotor-bearing system which consists of asymmetrical rigid disks, discrete isotropic bearings and non-uniform asymmetrical Rayleigh shafts, is given as (Jei and Lee, 1987; Lee and Jei, 1988)

$$L\phi_r = \lambda_r M\phi_r \quad \text{in } \tau \quad (1.a)$$

$$B_i \phi_r = 0 \quad i=1,2,\dots,p \text{ on } \sigma \quad (1.b)$$

$$r=1,2,3,\dots$$

where  $M, L$  and  $B_i$  represent the homogenous, linear, differential defined in terms of a system parameter  $E$ , and  $\phi_r$  denotes the system eigenfunction vector.  $L$  is of order  $2p$  while  $M$  and  $B_i$  are of order  $2p-1$  at most and  $M$  is positive definite over the range of  $E$ .  $\tau$  and  $\sigma$  denote the field and boundary in the eigenvalue problem. Any boundary conditions containing eigenvalues can be incorporated in the field equation (1.a) by extending the definitions of the operators and the eigenfunctions in Eq. (1) (Jei and Lee, 1987; Lee and Jei, 1988)

Let us define the inner product of two complex state vectors  $a = \{a_1, a_2\}^T$  and  $b = \{b_1, b_2\}^T$  as

$$\langle a, b \rangle = \langle a_1, b_1 \rangle + \langle a_2, b_2 \rangle \quad (2)$$

$$= \int_0^l \bar{b}_1 a_1 dx + \int_0^l \bar{b}_2 a_2 dx$$

where the bar denotes the complex conjugate. The adjoint eigenvalue problem associated with Eq. (1) is given by

$$\bar{\lambda}_s M^* \Psi_s = L^* \Psi_s \quad s=1,2,3,\dots \quad (3)$$

where  $M^*$  and  $L^*$  are the adjoints of  $M$  and  $L$ , respectively, and  $\Psi_s$  is the adjoint eigenfunction vector. When the damping effects of rotor-bearing systems are not considered,  $M^*$  and  $L^*$  are found to be (Jei and Lee, 1987; Lee and Jei, 1988)

$$M^* = M^T, \quad L^* = L^T \quad (4)$$

where  $T$  denotes transpose,  $\phi_r$  and  $\Psi_s$  may be biorthonormalized so as to satisfy

$$\langle M\phi_r, \Psi_s \rangle = \sigma_{rs} \quad (5)$$

$$\langle L\phi_r, \Psi_s \rangle = \lambda_r \sigma_{rs}$$

where  $\sigma_{rs}$  is the Kronecker delta. If  $k_{yz}(x) = -k_{zy}(x)$  in anisotropic rotor-bearing stems or  $\rho I_{yz}(x) = 0$  in asymmetrical rotor-bearing systems,  $\phi_r$  and  $\Psi_s$  satisfy the same eigenvalue problem (Jei and Lee, 1987; Lee and Jei, 1988), resulting in

$$\bar{\Psi}_{ry}(x) = K_r \phi_{ry}(x) \text{ and } \bar{\Psi}_{rz}(x) = -K_r \phi_{rz}(x) \quad (6)$$

where the constant  $K_r$  is to be determined from biorthonormality conditions.  $1/K_r$ , a complex quantity, is the so called modal norm.

The small variations in system parameter  $E$  produce a small perturbation in the operators  $L, M$  and  $q$  ( $0 \leq q \leq p$ ) boundary operators  $B_i$ . These operators become  $L = L_0 + \Delta L, M = M_0 + \Delta M$  and  $B_i = B_{i0} + \Delta B_i$  ( $i=1,2,\dots,q$ ), where  $\Delta L, M$  and  $\Delta B_i$  are the perturbation operators with norms of  $\epsilon$ . To evaluate the criteria of the curve veering in the eigenvalue problem, assume there exist two nearly equal eigenvalues  $\lambda_r^0$  and  $\lambda_s^0$  for the unperturbed problem. Perkins and Mote (1986) evaluated the perturbation solutions up to second order for  $\lambda_r$  and  $\lambda_s$  as

$$\lambda_r = \lambda_r^0 + c_r + d_r + x_{rs}/(\lambda_r^0 - \lambda_s^0) \quad (7)$$

$$\lambda_s = \lambda_s^0 + c_s + d_s + x_{sr}/(\lambda_s^0 - \lambda_r^0)$$

where

$$c_r = (k_{rr} - \lambda_r^0 m_{rr}), \quad d_r = m_{rr}(-k_{rr} + \lambda_r^0 m_{rr}),$$

$$x_{rs} = (k_{rs} - \lambda_r^0 m_{rs})(k_{sr} - \lambda_r^0 m_{sr})$$

$$k_{rs} = \langle \Delta L \phi_s^0, \Psi_r^0 \rangle_\tau + \sum_{i=1}^q \langle \Delta B_i \phi_s^0, \Psi_r^0 \rangle_\sigma,$$

$$m_{rs} = \langle \Delta M \phi_s^0, \Psi_r^0 \rangle_\tau$$

Note that  $x_{rs}$  and  $x_{sr}$  measure the coupling of the unperturbed eigenfunctions.

With the expansion of  $c_r, d_r$  and  $x_{rs}$  in Taylor series about  $E = E_0$ , Eq. (7) can be rewritten as (Perkins and Mote, 1986)

$$\lambda_r(\epsilon) = \lambda_r^0 + [D^1 c_r] \epsilon + \frac{1}{2} [D^2 c_r + D^2 d_r + D^2 x_{rs}/(\lambda_r^0 - \lambda_s^0)] \epsilon^2$$

$$\lambda_s(\epsilon) = \lambda_s^0 + [D^1 c_s] \epsilon + \frac{1}{2} [D^2 c_s + D^2 d_s + D^2 x_{sr}/(\lambda_s^0 - \lambda_r^0)] \epsilon^2 \quad (8)$$

where  $D^k = d^k/dE^k|E_0, k=1,2,\dots$ . When the eigenvalues are pure imaginary values, Eq. (8) can be rewritten as

$$\omega_r(\epsilon) = \omega_r^0 + \frac{1}{j} [D^1 c_r] \epsilon + \frac{1}{2j} [D^2 c_r + D^2 d_r] \epsilon^2 - \frac{1}{2} [D^2 x_{rs}/(\omega_r^0 - \omega_s^0)] \epsilon^2 \quad (9)$$

$$\omega_s(\epsilon) = \omega_s^0 + \frac{1}{j} [D^1 c_s] \epsilon + \frac{1}{2j} [D^2 c_s + D^2 d_s] \epsilon^2 - \frac{1}{2} [D^2 x_{sr}/(\omega_s^0 - \omega_r^0)] \epsilon^2$$

where  $\lambda_r = j\omega_r$ , and  $j$  and  $\omega$  are the imaginary unit and whirl natural frequency, respectively. When  $D^2 x_{rs}$ ,  $D^2 x_{sr}$  are not zero, the loci concavities depend strongly on separation  $|\omega_r^0 - \omega_s^0|$ . When the real values of  $D^2 x_{rs}$  and  $D^2 x_{sr}$  are both negative, the  $\omega_r(\epsilon)$  and  $\omega_s(\epsilon)$  loci veer away from each other as they approach. When the real values of  $D^2 x_{rs}$  and  $D^2 x_{sr}$  are both positive, the  $\omega_r(\epsilon)$  and  $\omega_s(\epsilon)$  loci veer towards each other as they approach. When the real values of  $D^2 x_{rs}$  and  $D^2 x_{sr}$  are of opposite sign, the concavities of the  $\omega_r(\epsilon)$  and  $\omega_s(\epsilon)$  loci are of the same sign. Then loci now veer with each other as they approach.

### 3. ANISOTROPIC ROTOR-BEARING SYSTEM

Consider an anisotropic rotor-bearing system consisting of flexible non-uniform Rayleigh shafts,  $D$  discrete rigid disks

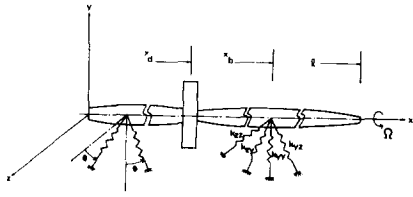


Fig. 1 Typical anisotropic rotor system

and  $B$  anisotropic bearings as shown in Fig. 1. The equations of motion including the effects of gyroscopic moment and rotary inertia are then expressed, in inertial coordinates, as (Lee and Jei, 1988; Jei, 1988)

$$\rho A(x) \frac{\partial^2 y}{\partial t^2} - \frac{\partial}{\partial x} \left[ J_T(x) \frac{\partial^3 y}{\partial x \partial t^2} \right] - \Omega \frac{\partial}{\partial x} \left[ J_p(x) \frac{\partial^2 z}{\partial x \partial t} \right] + \frac{\partial^2}{\partial x^2} \left[ EI(x) \frac{\partial^2 y}{\partial x^2} \right] + k_{yy}(x)y + k_{yz}(x)z = f_y(x,t) \quad (10.a)$$

$$\rho A(x) \frac{\partial^2 z}{\partial t^2} - \frac{\partial}{\partial x} \left[ J_T(x) \frac{\partial^3 z}{\partial x \partial t^2} \right] + \Omega \frac{\partial}{\partial x} \left[ J_p(x) \frac{\partial^2 y}{\partial x \partial t} \right] + \frac{\partial^2}{\partial x^2} \left[ EI(x) \frac{\partial^2 z}{\partial x^2} \right] + k_{zz}(x)z + k_{zy}(x)y = f_z(x,t) \quad (10.b)$$

$(0 < x < \ell)$

where

$$\rho A(x) = \rho A^e(x) + \sum_{d=1}^D m^d \delta(x - x_d)$$

$$J_T(x) = J_T^e(x) + \sum_{d=1}^D J_T^d \delta(x - x_d)$$

$$J_p(x) = J_p^e(x) + \sum_{d=1}^D J_p^d \delta(x - x_d)$$

$$k_{yy}(x) = \sum_{b=1}^B k_{yy}^b \delta(x - x_b), k_{yz}(x) = \sum_{b=1}^B k_{yz}^b \delta(x - x_b)$$

$$k_{zz}(x) = \sum_{b=1}^B k_{zz}^b \delta(x - x_b), k_{zy}(x) = \sum_{b=1}^B k_{zy}^b \delta(x - x_b)$$

and  $\rho A(x)$  is the mass per unit length,  $J_T(x)$  the diametral mass moment of inertia,  $J_p(x)$  the polar mass moment of inertia,  $EI(x)$  the flexural rigidity,  $m^d$  the disk mass,  $\ell$  the length of the rotor,  $\Omega$  the rotational speed,  $x$  the position coordinate along the shaft, and  $f_y(x,t), f_z(x,t)$  are the distributed forcing functions in the  $y$  and  $z$  directions, respectively. The superscript  $e$  denotes the shaft and,  $d$  and  $b$  denote the  $d$ -th rigid disk located at  $x = x_d$  and the  $b$ -th discrete bearing located at  $x = x_b$ , respectively.

The occurrence of curve veering is, first, checked with rotational speed variations. When  $\Omega = \Omega_0 + \Delta\Omega$ ,  $m_{sr}$  and  $k_{sr}$  in Eq. (7) are given, using Eq. (2), by

$$m_{sr} = \Delta\Omega \int_0^{\ell} J_p(x) \left[ \frac{\partial \bar{\Psi}_{sy}}{\partial x} \frac{\partial \phi_{rz}}{\partial x} - \frac{\partial \bar{\Psi}_{sz}}{\partial x} \frac{\partial \phi_{ry}}{\partial x} \right] dx \quad (11)$$

$$k_{sr} = 0$$

If  $k_{yz}(x) = k_{zy}(x) = 0$ , mode shapes become planar mode shapes and  $K_r$  of Eq. (6) becomes a pure imaginary value (Lee and Jei, 1988; Jei, 1988). When the mode shapes in  $y, z$  directions,  $\phi_{ry}$  and  $\phi_{rz}$ , are planar,  $\phi_{rz}$  is a pure imaginary valued function whereas  $\phi_{ry}$  is a real valued function. Let  $\phi_{rz} = j\phi_{rz}^R$  where  $\phi_{rz}^R$  is a real valued function. Then the  $D^2 x_{rs}$  in Eq. (9) is given by

$$D^2 x_{rs} = -(\omega_0^2)^2 [R_r \int_0^{\ell} J_p(x) \left( \frac{\partial \bar{\phi}_{sy}}{\partial x} \frac{\partial \phi_{rz}^R}{\partial x} - \frac{\partial \bar{\phi}_{ry}}{\partial x} \frac{\partial \phi_{sz}^R}{\partial x} \right) dx] \quad (12)$$

where  $K_r = jR_r$  and  $R_r$  is a real constant (Lee and Jei, 1988; Jei, 1988). Since  $D^2 x_{rs}$  and  $D^2 x_{sr}$  are both negative, as shown in Eq. (12), the  $\omega_r$  and  $\omega_s$  loci veer away from each other as they approach.

The curve veering in the whirl natural frequency of an isotropic rotor-bearing system as rotational speed varies was shown by Crandall and Yeh (1989). They treated a single spool machine with the uniform rotor rotating in the uniform stator supported by isotropic springs. Since the rotor-bearing system is symmetric about the midplane, the whirling modes can be divided into two families: even modes; i.e., modes symmetrical about the midplane, and odd modes; i.e., modes anti-symmetrical about the midplane. They reported that "It is interesting that when the curve for an odd rotor mode approaches the curve for an even stator mode, or an even rotor mode approaches an odd stator mode, there is no coupling between the modes and curve intersect, each oblivious to the presence of the other. On the other hand when the curve for an even rotor mode approaches the curve for an

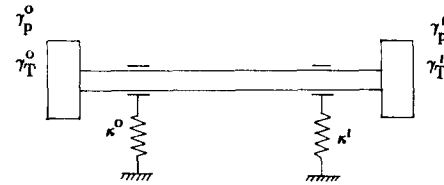
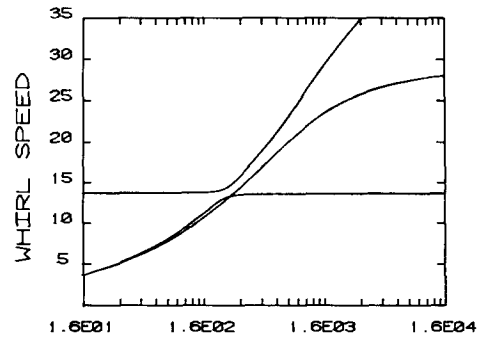
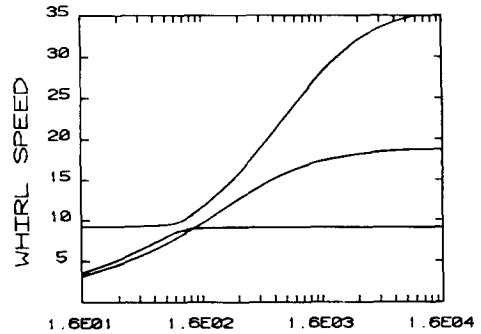


Fig. 2 Uniform shaft with two tip disks



(a) Forward whirl speeds



(b) Backward whirl speeds

Fig. 3 Whirl speeds of the shaft with two tip disks as bearing coefficient varies ( $c = 20, r = 0.02, \gamma_r^0 = \gamma_r^1 = 0.002, \gamma_b^0 = \gamma_b^1 = 0.004$ )

even stator mode, or an odd rotor mode approaches an odd stator mode, the two modes form a coupled system and the curves repel each other avoiding an intersection." The reason can be explained by Eq. (12). Between even and odd modes the integration of Eq. (12) is zero. Therefore there is no coupling between the modes. But between even(odd) and even(odd) modes, the integration of Eq. (12) is positive real value, and the curve veering between the modes occur.

When the bearings are isotropic, that is,  $k_{yy}=k_{zz}=k$  and  $k_{yz}=k_{zy}=0$ , the mode shapes in  $y$  and  $z$  directions are identical. As the stiffness coefficients of bearings vary, the

occurrence of curve veering is checked. When  $k=k_0+\Delta k$ , the  $x_{rs}$  in Eq. (7) is given by

$$x_{rs} = -[R_r \int_0^l \Delta k \phi_s \phi_r dx]^2 \quad (13)$$

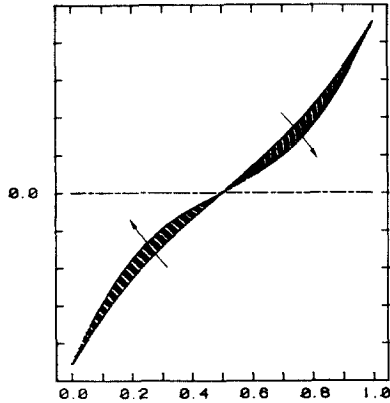
where  $\phi_r = \phi_{ry} + j\phi_{rz}$ . Since  $D^2 x_{rs} (= D^2 x_{sr})$  is negative, the  $\omega_r$  and  $\omega_s$  loci veer away from each other as they approach.

Consider an isotropic rotor-bearing system which consists of a uniform Rayleigh shaft, two tip disks and two isotropic bearings as shown in Fig. 2. The rotor is symmetric about the midplane. The solution procedures are given in (Lee and Jei, 1988; Jei, 1988). For convenience let introduce the nondimensional variables of  $r$  (radius of gyration),  $c$  (rotational speed),  $\beta$  (mass of tip disk),  $\gamma_T$  and  $\gamma_p$  (diametral and polar mass moment of inertia of tip disk), and  $k$  (bearing stiffness) (Lee and Jei, 1988; Jei, 1988). When  $c=20$ ,  $r=0.02$ ,  $\beta^o = \beta^l = 0.7$ ,  $\gamma_T^o = \gamma_T^l = 0.002$  and  $\gamma_p^o = \gamma_p^l = 0.004$ , whirl speeds are plotted against bearing stiffness  $k$  in Fig. 3. In the veering region of forward whirl the mode shape variations are shown in Fig. 4. In Fig. 4 the broken lines show mode shape variations as the stiffness is increased by a given amount. As shown in Fig. 3, the curve veering occurs as  $\omega_2$  approaches to  $\omega_3$ . But when  $\omega_1$  approaches to  $\omega_2$  or  $\omega_3$ , any coupling between  $\omega_1$  and  $\omega_2$  or  $\omega_3$  does not occur. As shown in Fig. 4, the 1st mode is an odd mode, whereas the 2nd and 3rd modes are even modes. Therefore the coupling factors between the odd (the 1st mode) and even (the 2nd and 3rd mode) modes,  $x_{12}$  and  $x_{13}$  in Eq. (13), are zero. During veering the 2nd mode shape changes to the 3rd mode shape, the 3rd mode shape to the 2nd mode shape, respectively, in a rapid but continuous way. But the 1st mode shape slowly changes during crossing.

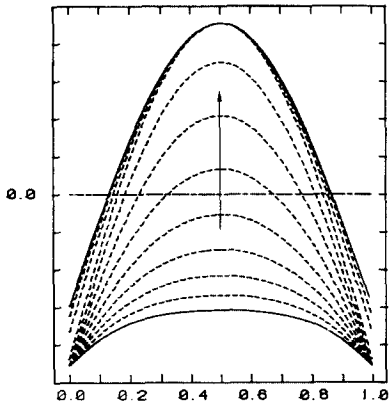
#### 4. ASYMMETRICAL ROTOR-BEARING SYSTEMS

Consider an asymmetrical rotor-bearing system consisting of flexible non-uniform asymmetrical Rayleigh shafts,  $D$  rigid asymmetrical disks and  $B$  isotropic bearings. Since the governing equations of asymmetrical rotor systems in stationary coordinates,  $S: oxyz$ , are of periodically varying coefficients, the equations of motion are conveniently expressed in rotating coordinates,  $R: OXYZ$ , defined relative to the  $S: oxyz$  by a single rotation  $\Omega t$  about  $x$  axis. The equations of motion of the asymmetrical rotor-bearing system including the effects of gyroscopic moments and rotary inertia are in the inertial coordinates as (Jei and Lee, 1987; Jei, 1988),

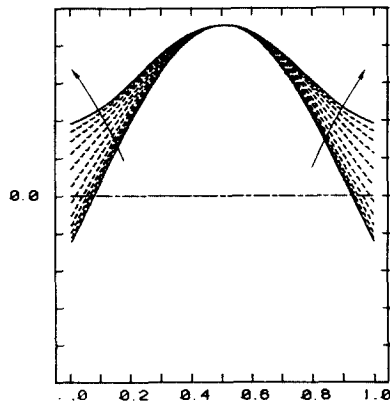
$$\begin{aligned} & \rho A(X) \frac{\partial^2 Y}{\partial t^2} + \frac{\partial}{\partial X} \left( \rho I_x \frac{\partial^3 Y}{\partial X \partial t^2} \right) - \frac{\partial}{\partial X} \left( \rho I_{yz} \frac{\partial^3 Z}{\partial X \partial t} \right) \\ & - 2\Omega \rho A(X) \frac{\partial Z}{\partial t} \\ & - \Omega \frac{\partial}{\partial X} \left( \rho I_0 \frac{\partial^2 Z}{\partial X \partial t} \right) + \frac{\partial^2}{\partial X^2} \left( EI_x \frac{\partial^2 Y}{\partial X^2} \right) \\ & + \frac{\partial^2}{\partial X^2} \left( EI_{yz} \frac{\partial^2 Z}{\partial X^2} \right) + k(X) Y - \Omega^2 \left[ \rho A(X) Y \right. \\ & \left. + \frac{\partial}{\partial X} \left\{ (\rho I_x - \rho I_y) \frac{\partial Y}{\partial X} + \rho I_{yz} \frac{\partial Z}{\partial X} \right\} \right] = q_y \quad (14) \\ & \rho A(X) \frac{\partial^2 Z}{\partial t^2} + \frac{\partial}{\partial X} \left( \rho I_y \frac{\partial^3 Z}{\partial X \partial t^2} \right) - \frac{\partial}{\partial X} \left( \rho I_{yz} \frac{\partial^3 Y}{\partial X \partial t} \right) \\ & + 2\Omega \rho A(X) \frac{\partial Y}{\partial t} - \Omega \frac{\partial}{\partial X} \left( \rho I_0 \frac{\partial^2 Y}{\partial X \partial t} \right) + \frac{\partial^2}{\partial X^2} \\ & \left( EI_y \frac{\partial^2 Z}{\partial X^2} \right) + \frac{\partial^2}{\partial X^2} \left( EI_{yz} \frac{\partial^2 Y}{\partial X^2} \right) + k(X) Z \end{aligned}$$



(a) The 1st mode shape variations



(b) The 2nd mode shape variations



(c) The 3rd mode shape variations

Fig. 4 Mode shape variations during curve veering ( $c=20$ ,  $r=0.02$ ,  $\gamma_T^o = \gamma_T^l = 0.002$ ,  $\gamma_p^o = \gamma_p^l = 0.004$ )

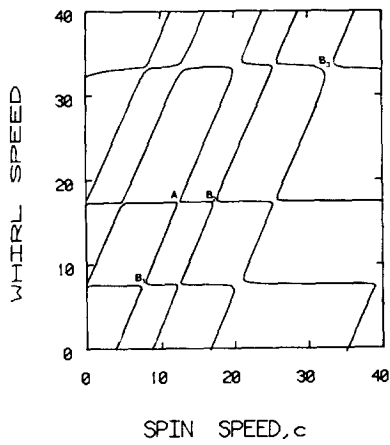


Fig. 5 Whirl speeds of the asymmetrical shaft supported by isotropic bearings  
 ( $\gamma^2=0.000333, \epsilon=1.4, k^0=40, k^1=80$ )

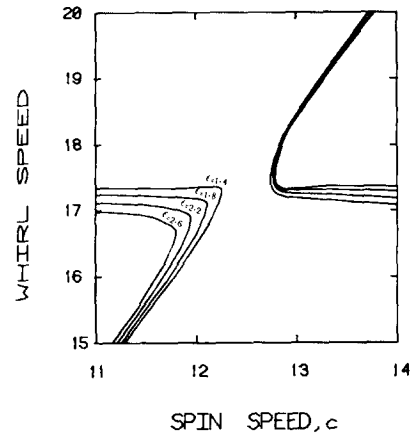
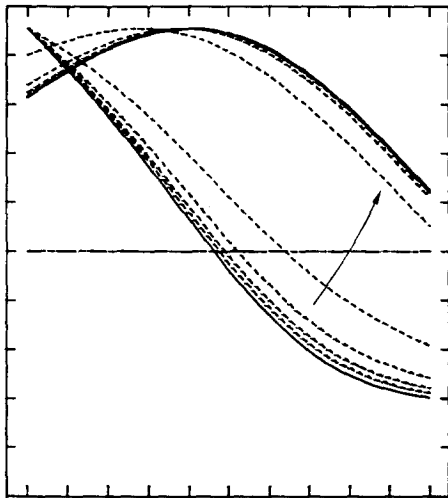
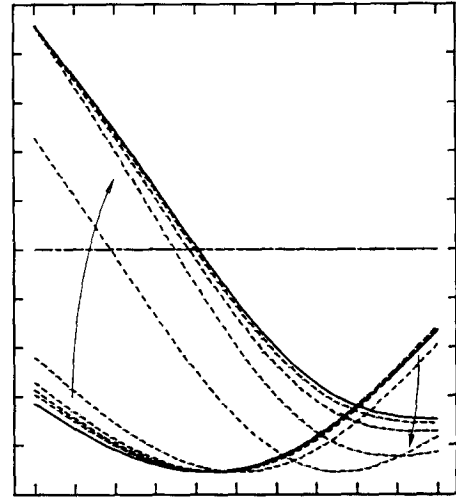


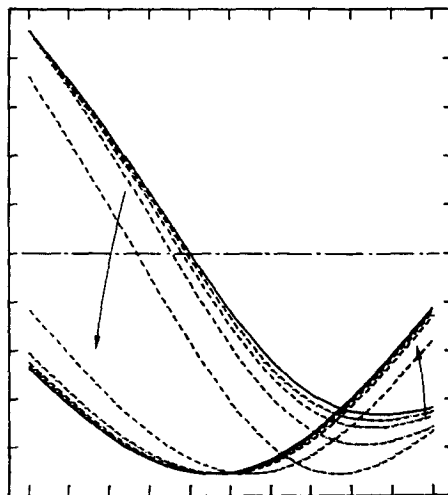
Fig. 6 Whirl speeds near the region A as shaft asymmetry varies  
 ( $\gamma^2=0.000333, \epsilon=1.4, k^0=40, k^1=80$ )



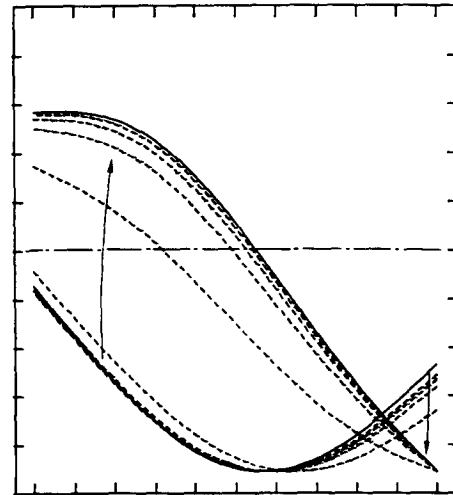
(a) Variations of the 2nd mode shape to the 1st mode shape  
 (Y direction)



(c) Variations of the 1st mode shape to the 2nd mode shape  
 (Y direction)



(b) Variations of the 2nd mode shape to the 1st mode shape  
 (Z direction)



(d) Variations of the 1st mode shape to the 2nd Mode shape  
 (Z direction)

Fig. 7 Mode shape variations during curve veering  
 ( $\gamma^2=0.000333, \epsilon=1.4, k^0=40, k^1=80$ )

$$\begin{aligned}
 & -\Omega^2 \left[ \rho A(X)Z + \frac{\partial}{\partial X} \{ (\rho I_x - \rho I_z) \frac{\partial Z}{\partial X} \right. \\
 & \left. + \rho I_{yz} \frac{\partial Y}{\partial X} \right] = q_z \\
 & (0 < X < \ell)
 \end{aligned}$$

where

$$\begin{aligned}
 \rho A(X) &= \rho A^e(X) + \sum_{d=1}^D m^d \delta(X - X_d), \\
 \rho I_x(X) &= \rho I_x^e(X) + \sum_{d=1}^D \rho I_x^d \delta(X - X_d) \\
 \rho I_y(X) &= \rho I_y^e(X) + \sum_{d=1}^D \rho I_y^d \delta(X - X_d), \\
 \rho I_z(X) &= \rho I_z^e(X) + \sum_{d=1}^D \rho I_z^d \delta(X - X_d), \\
 \rho I_{yz}(X) &= \rho I_{yz}^e(X) + \sum_{d=1}^D \rho I_{yz}^d \delta(X - X_d), \\
 k(X) &= \sum_{b=1}^B k^b \delta(X - X_b) \\
 \rho I_0(X) &= \rho I_x(X) - \rho I_y(X) - \rho I_z(X)
 \end{aligned} \quad (15)$$

and  $\rho A(X)$  is the mass per unit length,  $\rho I_x(X)$ ,  $\rho I_y(X)$ ,  $\rho I_z(X)$  and  $\rho I_{yz}(X)$  the mass moments of inertia about  $X$ ,  $Y$  and  $Z$  axes, respectively, and  $m^d$  the disk mass,  $\ell$  the length of the rotor,  $\Omega$  the rotational speed, and  $q_y(x, t)$ ,  $q_z(x, t)$  are the distributed forcing functions in the  $y, z$  directions, respectively.  $EL_y$ ,  $EL_z$  are the flexural shaft rigidity about  $Y, Z$  axes, respectively.

As rotational speed varies, the occurrences of the curve veering in the eigenvalue problem of asymmetrical rotor-bearing systems are checked. If  $\rho I_{yz}(X) = 0$ , mode shapes become planar mode shapes and  $K_r$  of Eq. (6) becomes a pure imaginary value (Jei and Lee, 1987; Jei, 1988). When the mode shapes in  $Y, Z$  directions,  $\phi_{ry}$  and  $\phi_{rz}$ , are planar,  $\phi_{rz}$  is a pure imaginary function whereas  $\phi_{ry}$  is a real valued function.

When  $\Omega = \Omega_0 + \Delta\Omega$ , the  $m_{rs}$  and  $k_{rs}$  in Eq. (7) are given by

$$\begin{aligned}
 m_{rs} &= \Delta\Omega R_r \left[ \int_0^{\ell} 2\rho A (\phi_{sy} \phi_{rz}^R + \phi_{sz}^R \phi_{ry}) dX \right. \\
 & \left. - \int_0^{\ell} \rho I_0 \left( \frac{\partial \phi_{sz}^R}{\partial X} \frac{\partial \phi_{ry}}{\partial X} + \frac{\partial \phi_{sy}}{\partial X} \frac{\partial \phi_{rz}^R}{\partial X} \right) dX \right] \\
 k_{rs} &= j(\Delta\Omega^2 + 2\Omega_0 \Delta\Omega) R_r \left[ \int_0^{\ell} \rho A (\phi_{sy} \phi_{ry} + \phi_{sz}^R \phi_{rz}^R) dX \right. \\
 & \left. - \int_0^{\ell} (\rho I_x - \rho I_y) \frac{\partial \phi_{sy}}{\partial X} \frac{\partial \phi_{ry}}{\partial X} dX - \int_0^{\ell} (\rho I_x - \rho I_z) \right. \\
 & \left. \frac{\partial \phi_{sz}^R}{\partial X} \frac{\partial \phi_{rz}^R}{\partial X} dX \right] = jk_{rs}^R
 \end{aligned} \quad (16)$$

where  $m_{rs}$  and  $k_{rs}^R (= k_{sr}^R)$  are real constants, and  $\phi_{rz} = j\phi_{rz}^R$  where  $\phi_{rz}^R$  is a real valued function. Therefore the coupling factor  $x_{sr}$  in Eq. (7)

$$x_{rs} = -(k_{rs}^R - \omega_r^0 m_{rs})(k_{sr}^R - \omega_r^0 m_{sr}) \quad (17)$$

Since  $D^2 x_{sr}$  is negative,  $\omega_r$  and  $\omega_s$  loci veer away from each other as they approach.

Now we consider two examples of the uniform asymmetrical shaft supported by isotropic bearings at ends and the cantilever shaft with a tip disk. Solution procedures are given in (Jei and Lee, 1987; Jei, 1988). For convenience let introduce nondimensional variables of  $\epsilon (= I_z/I_y, \text{shaft asymmetry})$ ,  $\gamma_e, \gamma_n$  and  $\gamma_{en}$  (non-dimensional mass moment of inertia of tip disk).

(1) Isotropic Spring Support

When a uniform asymmetrical shaft is supported by

isotropic bearings at its ends ( $\chi = 0, 1$ ), the whirl speeds in stationary coordinates are shown in Fig. 5. The whirl speeds near the region A are also shown in Fig. 6 as the shaft asymmetry,  $\epsilon$ , varies. Near the curve veering region A the mode shape changes are shown in Fig. 7. During veering the 2nd mode shape abruptly changes to the 1st mode shape as shown in Fig. 7(a) and 7(b), and the 1st mode shape to the 2nd mode shape as shown in Fig. 7(c), and 7(d), respectively. As discussed in (Jei and Lee, 1987; Jei, 1988) once a solution for whirl speed,  $\omega$ , found,  $-\omega$  become another solution, that is, complex conjugate relations. And the mode shapes associated with  $\omega$  and  $-\omega$  should be a complex conjugate pair. Therefore near the regions  $B_1, B_2$  and  $B_3$ , i.e., so called major unstable regions which are bounded by major critical speeds, the mode shapes do not severely change although curve veerings occur.

(2) Cantilever Beam with a Tip Disk

The cantilever shaft with a tip disk is shown in Fig. 8. When the principal axes of the asymmetrical tip disk are coincident with the principal axes of the cantilever shaft, that is, the relative orientation angle between the principal axes of the shaft and disk,  $\theta$ , is zero, the mode shapes are planar. If  $\theta \neq 0$ ,  $\phi_e(\chi)$  and  $\phi_n(\chi)$  become non-planar. The whirl speeds of the cantilever shaft with a tip disk are shown in Fig. 9 when  $\theta = 45^\circ$ . The mode shape changes during the veering near the

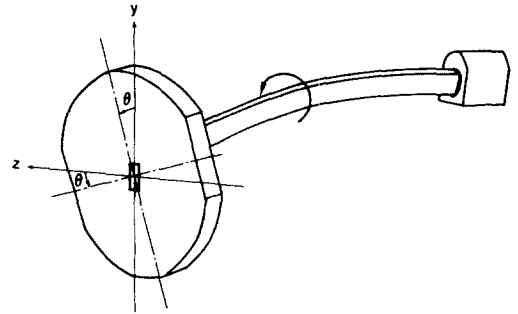


Fig. 8 Asymmetrical cantilever shaft with a tip disk

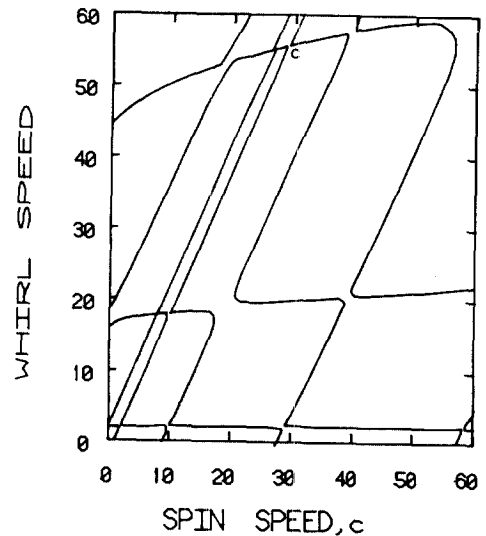


Fig. 9 Whirl speeds of asymmetrical cantilever shaft with a tip disk

$$\gamma^2 = 0.00033, \quad \epsilon = 1.4, \quad \beta^1 = 0.7, \quad \gamma_e^1 = 0.001667, \quad \gamma_n^1 = 0.00233$$

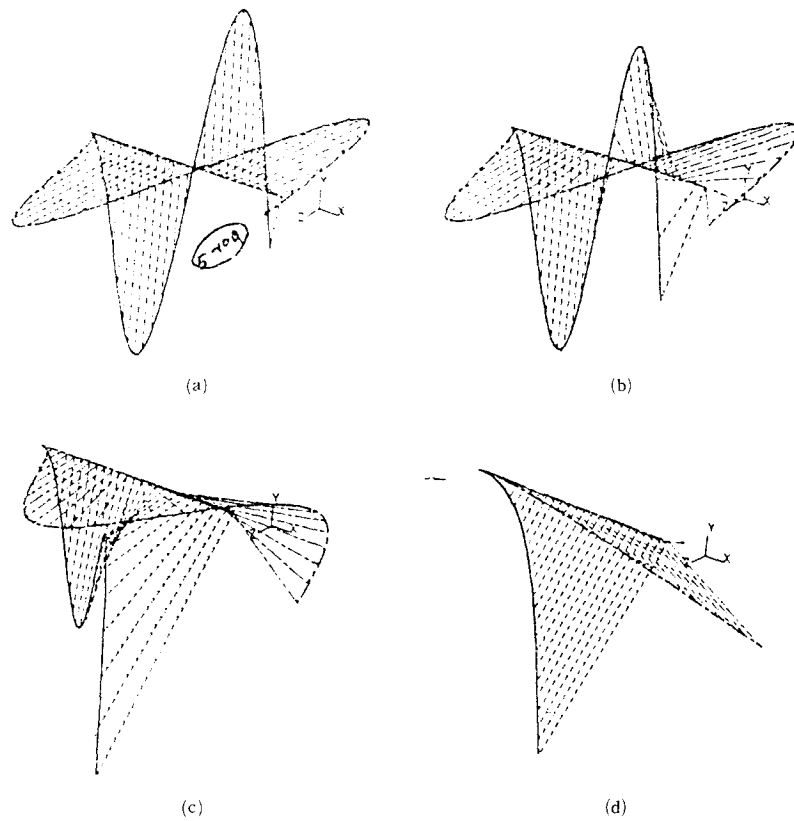


Fig. 10 Variations of the 3rd mode shape to the 1st mode shape during curve veering

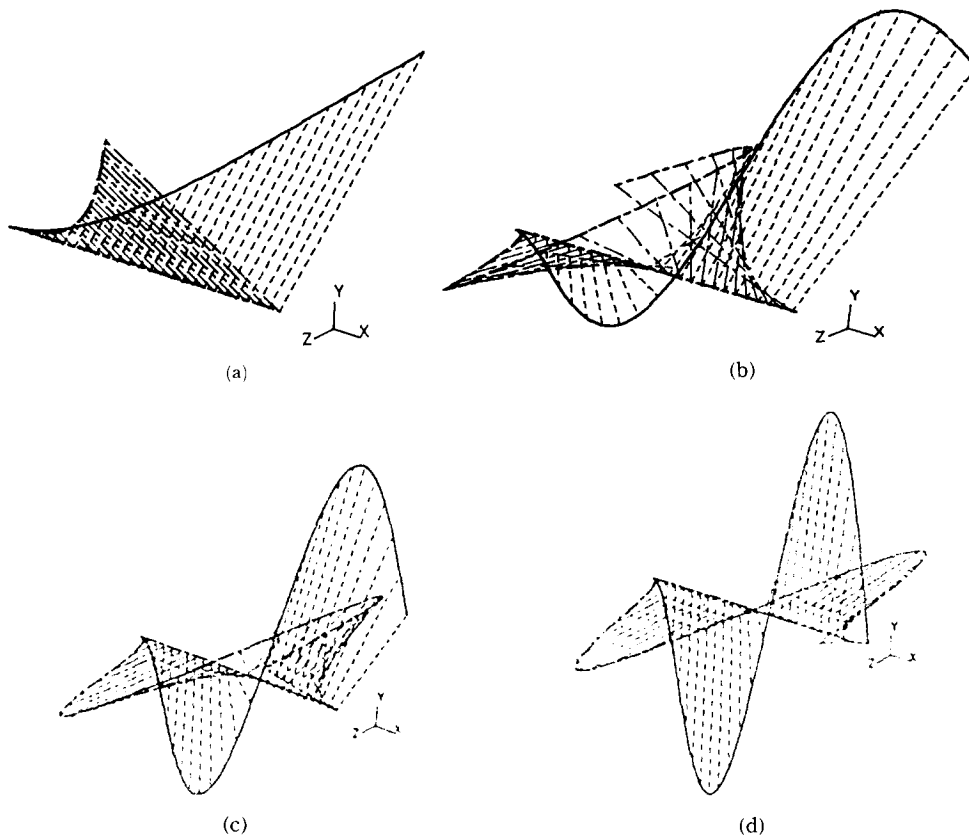


Fig. 11 Variations of the 1st mode shape to the 3rd mode shape during curve veering

region  $C$  are shown in Figs. 10 and 11. During the veering the 3rd mode shape abruptly changes to the 1st mode shape as shown in Figs. 10(a) ~ 10(d), and the 1st mode shape to the 3rd mode shape as shown in Figs. 11(a) ~ 11(d), respectively. As shown in Figs. 10, and 11, the mode shapes change in a rapid but continuous way.

## 5. CONCLUSIONS

The existence of the curve veering in the eigenvalue problem of rotor-bearing systems including the effects of gyroscopic moments and rotary inertia is verified using the modal analysis and exact solution methods developed by authors (Jei and Lee, 1987; Lee and Jei, 1988; Jei, 1988) and the perturbation technique developed by Perkins and Mote (1986). The criteria of the curve veering are derived as the bearing stiffness and rotational speed vary. The abrupt but continuous changes of the mode shapes during veering are also illustrated.

## REFERENCES

- Claassen, R.W. and Thorne, C.J., 1962, "Vibrations of Rectangular Cantilever Plate," *J. of Aerospace Sci.*, Vol. 29., pp. 1300~1305.
- Crandall, S.H. and Yeh, N.A., 1989, "Automatic Generation of Component Modes for Rotordynamic Substructures," *J. of Vibration, Acoustics, Stress, and Reliability in Design*, Vol. 111, pp. 6~10.
- Dimentberg, F.M., 1961, "Flexural Vibration of Rotating Shaft," translated from Russian by Production Engineering Research Association, Butterworths, London.
- Jei, Y.G. and Lee, C.W., 1987, "Modal Analysis of Continuous Asymmetrical Rotor-Bearing Systems," KSME Meeting, Dynamics and Control Division, Accepted for Publication in *Journal of Sound and Vibration*.
- Jei, Y.G., 1988, "Modal Analysis of Continuous Asymmetrical Rotor-Bearing Systems," Ph. D. Dissertation, KAIST.
- Jei, Y.G. and Lee, C.W., 1989, "Vibrations of Anisotropic Rotor-Bearing Systems," Twelfth Biennial ASME Conference on Mechanical Vibration and Noise, Montreal, Canada, September.
- Kuttler, J.R. and Sigillito, V.G., 1981, "On Curve Veering," *J. of Sound and Vibration*, Vol. 75, pp. 585~588.
- Leissa, A.W., 1974, "On a Curve Veering Abberation," *J. of Applied Mathematics and Physics (ZAMP)*, Vol. 25, pp. 99~111.
- Lee, C.W. and Jei, Y.G., 1988, "Modal Analysis of Continuous Rotor-Bearing Systems," *J. of Sound and Vibration*, Vol. 126, pp. 345~361.
- Perkins, N.C. and Mote, C.D., Jr., 1986, "Comments on Curve Verring in Eigenvalue Problems," *J. of Sound and Vibration*, Vol. 106, pp. 451~463.
- Schajer, G.S., 1984, "The Vibration of a Rotating Circular String Subject to a Fixed End Restraint," *J. of Sound and Vibration*, Vol. 92, pp. 11~19.
- Yamamoto, T. and Ota, H., 1964, "On the Unstable Vibrations of a Shaft Carrying an Unsymmetrical Rotor," *J. of Applied Mechanics*, pp. 515~552.